Electrophysiological Study of *Drosophila* Rhodopsin Mutants

EDWIN C. JOHNSON and WILLIAM L. PAK

From the Department of Biological Sciences, Purdue University, West Lafayette, Indiana 47907

ABSTRACT Electrophysiological investigations were carried out on several independently isolated mutants of the *ninaE* gene, which encodes opsin in R1–6 photoreceptors, and a mutant of the *ninaD* gene, which is probably important in the formation of the rhodopsin chromophore. In these mutants, the rhodopsin content in R1–6 photoreceptors is reduced by 10^2–10^6-fold. Light-induced bumps recorded from even the most severely affected mutants are physiologically normal. Moreover, a detailed noise analysis shows that photoreceptor responses of both a *ninaE* mutant and a *ninaD* mutant follow the adapting bump model. Since any extensive rhodopsin-rhodopsin interactions are not likely in these mutants, the above results suggest that such interactions are not needed for the generation and adaptation of light-induced bumps. Mutant bumps are strikingly larger in amplitude than wild-type bumps. This difference is observed both in *ninaD* and *ninaE* mutants, which suggests that it is due to severe depletion of rhodopsin content, rather than to any specific alterations in the opsin protein. Lowering or buffering the intracellular calcium concentration by EGTA injection mimics the effects of the mutations on the bump amplitude, but, unlike the mutations, it also affects the latency and kinetics of light responses.

INTRODUCTION

The first step in the excitation of a retinal photoreceptor is the absorption of a photon by the visual pigment molecule, rhodopsin. In both vertebrate rods and many invertebrate photoreceptors, single photons have been shown to generate electrophysiologically observable responses (Fuortes and Yeandle, 1964; Baylor et al., 1979). These single photon responses were first observed in *Limulus* and were named "quantum bumps." Rushton (1961) proposed that these bumps may be the elementary units of the receptor potential. Subsequently, Dodge et al. (1968) formulated a quantitative model, called the adapting bump model, relating quantum bumps to the receptor potential. Their model, which was later elaborated by others (e.g., Wong and Knight, 1980; Wong et al., 1982), states (*a*) that a summation of bumps gives rise to the light-induced conductance changes that underlie the generation of the receptor potential, and (*b*) that the

Address reprint requests to Dr. William L. Pak, Dept. of Biological Sciences, Purdue University, West Lafayette, IN 47907. Dr. Johnson's present address is Dept. of Biology, Brandeis University, Waltham, MA 02254.

J. GEN. PHYSIOL. © The Rockefeller University Press · 0022-1295/86/11/0651/23 $1.00

Volume 88 November 1986 651–673

basic mechanism of light adaptation is the decrease in the average amplitude of a bump with increasing light intensity. It has been shown in a number of animals that a bump is generated as a result of an effective absorption of a single photon by rhodopsin (Yeandle and Spiegler, 1973; Lillywhite, 1977). However, the detailed mechanism by which the bump is generated is not understood, nor is it known what other roles besides photon absorption rhodopsin might play in the generation and modulation of bumps. In this work, we have investigated the possible influence of rhodopsin on the physiological parameters of bumps using mutations that drastically reduce the rhodopsin content in the photoreceptors.

The mutations were isolated in chemical mutagenesis using the absence of the prolonged depolarizing afterpotential (PDA) in the electroretinogram (ERG) as

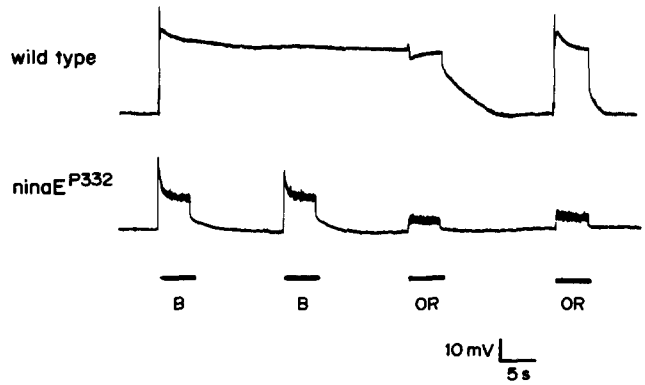

FIGURE 1. The PDA recorded intracellularly from a wild-type and a *ninaE* R1–6 photoreceptor. The first blue stimulus of 5 s duration induced the PDA in a wild-type photoreceptor (top trace). A second blue stimulus did not generate a further depolarization, which indicates that the photoreceptor was inactivated. An orange stimulus reversed the PDA. The same stimulus protocol induced neither the afterpotential nor the inactivation in *nina* mutants (bottom trace; $ninaE^{P332}$ is seen here). Note the large light-induced noise superimposed on the *ninaE* responses.

an assay (Pak, 1979). The PDA has been observed in every invertebrate photoreceptor investigated to date whenever a colored stimulus has been used to convert a substantial net amount of rhodopsin to metarhodopsin (Nolte et al., 1968; Cosens and Briscoe, 1972; Hillman et al., 1972; Brown and Cornwall, 1975). Unlike the light-coincident receptor potential, which is observed during a light stimulus, the PDA persists after the cessation of the stimulus and is terminated by photoisomerizing metarhodopsin back to rhodopsin. During a fully developed PDA, the photoreceptor fails to respond to additional PDA-inducing stimuli (Fig. 1, top trace), i.e., it is inactivated. Because the PDA requires a substantial net shift in the absolute amount of rhodopsin to metarhodopsin, the PDA is underdeveloped or absent in mutants with a drastically reduced amount of rhodopsin (Fig. 1, bottom trace). Mutants with this phenotype have been named *nina* (neither inactivation nor afterpotential). Eight *nina* genes (*ninaA*, *ninaB* . . . *ninaH*) have been identified to date from such mutations.

There are several classes of photoreceptors (R1–6, R7, R8) in the *Drosophila* compound eye. The photoreceptors of the major class, R1–6, all contain the same rhodopsin, and the minor classes of photoreceptors contain different kinds of rhodopsin (Harris et al., 1976; Hardie, 1979). It is estimated that the rhodopsin contained in R1–6 cells comprises >90% of all visual pigments present in the eye. All *nina* mutations were isolated on the basis of defects in the PDA generated by R1–6 cells. Thus, in this article, we refer only to rhodopsin in R1–6 photoreceptors.

Mutations at two different *nina* genes, *ninaD* and *ninaE*, were used in this work. Scavarda et al. (1983) had suggested previously that the *ninaE* gene probably encodes the major class of opsin in R1–6 photoreceptors on the basis of genetic evidence. Recent molecular isolation and sequencing of the gene has unequivocally established that the *ninaE* gene indeed codes for this opsin (O'Tousa et al., 1985; Zuker et al., 1985). The *ninaD* gene, on the other hand, is apparently involved in retinoid uptake or metabolism (Stephenson et al., 1983). A mutation in this gene thus reduces the rhodopsin content by limiting the amount of retinoids available for the formation of rhodopsin chromophore. These two classes of *nina* mutants were chosen because they affect the amount of rhodopsin by two very different mechanisms.

MATERIALS AND METHODS

Mutants Used

Both the control and mutant stocks were derived from the Oregon R wild-type strain of the fruitfly, *Drosophila melanogaster*. The mutants *ninaE* and *ninaD* were isolated in chemical mutagenesis of the wild-type flies, as described by Pak (1979). Both the control and mutant flies were made homozygous for the mutation white (*w*) (Lindsley and Grell, 1968) to eliminate the screening pigments in the eye, thereby increasing the sensitivity of the photoreceptor to light. Throughout this article, the control flies are referred to as "wild type." The *ninaE* gene is located on the third chromosome and has been cytogenetically localized to 92B5,6 on the polytene chromosomes (O'Tousa et al., 1985), and the *ninaD* gene is on the second chromosome and localized to 36D1-F1,2 (Pye, Q., unpublished data cited in Steward and Nusslein-Volhard, 1986).

Intracellular Recordings

For intracellular recording experiments, a 4-d-old female fly was mounted on its side on a glass slide using a mixture of myristic acid and beeswax. A small portion of the cornea was sliced off with a vibrating razor blade, inert vacuum grease was applied to the hole to prevent dessication, and a recording electrode was introduced into the hole. An animal so prepared would yield good recordings for several hours. The intracellular recording electrodes had a resistance of 100–150 MΩ when filled with 2 M potassium acetate (KAc) or 2 M KCl. The reference electrode was filled with saline and placed with its tip in the photoreceptor layer. Under these conditions, any interference from extracellular currents in the eye tissue was negligible.

The fly was dark-adapted for 5–10 min before each measurement. Only records that drifted by no more than 3 mV and had a good signal-to-noise ratio were used in noise analysis. Because of these requirements and the difficulty in holding a cell long enough for the analysis (0.5–1 h), <5% of the records were accepted for analysis. Signals were

filtered at 100 Hz with a steep-roll-off, six-pole Bessel low-pass filter in all but the capacitance measurement experiments and the EGTA experiment illustrated in Fig. 9. They were monitored on an oscilloscope, recorded on a pen recorder and FM tape, and analyzed by and stored in a PDP 11/03 laboratory computer (Digital Equipment Corp., Maynard, MA).

Measurement of Passive Electrical Properties

Voltage signals generated by current pulses of +0.1 nA injected into the cell were used to determine both the input resistance and the membrane time constant. An example of signals obtained from wild type and a mutant is shown in Fig. 2. The input resistance was obtained from the magnitude of the voltage drop across the membrane, determined using

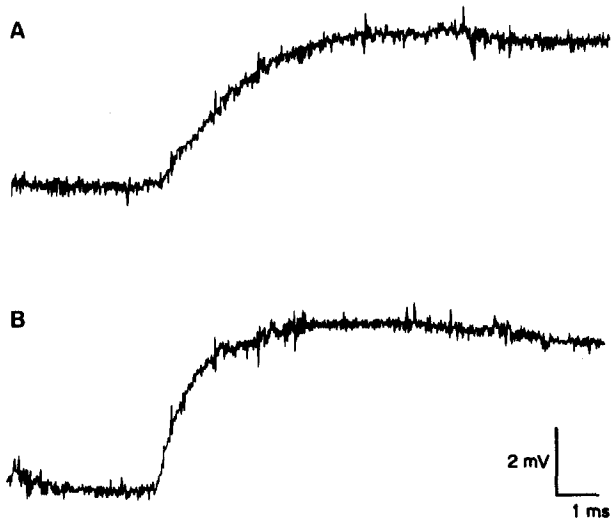

FIGURE 2. Sample traces used in the determination of the input resistance and membrane time constant. The signals were generated from the wild-type (*A*) and *ninaE*^{P334} (*B*) photoreceptors by a +0.1-nA, 500-ms current injection.

the bridge circuit of the preamplifier (model M4-A, W-P Instruments, Inc., New Haven, CT), and the membrane time constant was determined from the rise time of the voltage signal. The membrane capacitance was then calculated from the above two experimentally determined quantities.

Rall (1960) has pointed out that for a nonspherical neuron with dendritic branches, an estimate of the membrane time constant from 1/e of the voltage transient can lead to a significant underestimation, and he has developed a formalism for dealing with dendrite-dominated neurons. We chose not to apply his treatment to the present case for the following reasons. For our purposes, the absolute values of the time constant are not too important. The membrane time constants are used to calculate the membrane capacitances and then estimate the membrane surface areas of the mutants relative to those of wild type. The errors introduced by the geometry of the neuron should affect both wild type and the mutants and hence should have little or no effect on relative values. Also, the membrane surface area for wild type derived from the present measurements is remarkably close to the corresponding histological estimate (see Discussion), which suggests that the error introduced by our approach is not too serious.

Light Stimulus

A 150-W xenon arc lamp was used as the light source. The unattenuated illuminance at the eye level was 8.0×10^{16} photons/cm^2·s as determined by a digital photometer (J16, Tektronix, Inc., Beaverton, OR) at 500 nm over a 100-nm bandwidth. It was very difficult to determine the fraction of light reaching the rhabdomere and the fraction absorbed by the visual pigment. Experiments with several dissected corneas showed that the cornea acted as an ~0.8-log-unit neutral density filter. Thus, the illuminance at the photoreceptor was taken to be $\sim 1.3 \times 10^{16}$ photons/cm^2·s.

Electrophysiological Estimate of the Rhodopsin Content

The rhodopsin content in the photoreceptor was estimated by determining the light intensity necessary to induce, on the average, one bump. For the purpose of this study, a failure rate of one-third to two-thirds was taken as induction of one bump. Results were rejected if the average number of bumps to a given stimulus was not constant throughout an experiment within 90% confidence limit. Stimuli, filtered with a 520-nm cut-on filter, had a duration of 5 ms. The flash intensity was determined before each experiment.

The following expression, derived by Lisman and Bering (1977), was used to calculate the absolute number of rhodopsin molecules in a single photoreceptor cell from the stimulus intensity determined as described above:

$$R = N(0.001)/(2.3)\gamma\epsilon I,$$

where N is Avogadro's number, γ is the quantum efficiency of isomerization, ϵ is the extinction coefficient of rhodopsin, and I is the intensity of light needed to induce one bump. This relationship is based on Beer's law and on the assumptions that one effectively absorbed quantum yields one bump and that the photoreceptor contains a dilute solution of randomly oriented rhodopsin molecules.

The assumption of a dilute solution is valid for the mutants but not for wild type, and the assumption of randomly oriented absorbing molecules is invalid for both wild type and the mutants. Errors caused by these assumptions are estimated as below. The assumption of a dilute solution allowed Lisman and Bering (1977) to replace $\ln I_i/I_t$ by $(I_i - I_t)/I_i$ in the expressions for Beer's law, where I_i is the incident light intensity and I_t is the transmitted light intensity. From the absorbance by a wild-type rhabdomere estimated in the Appendix, i.e., $\Delta A = \log I_i/I_t \approx 0.27$, it can be shown that the above approximation leads to an underestimation of wild-type pigment concentration by ~26%. Because this error affects the relative rhodopsin content between wild type and mutants, an appropriate correction was incorporated into the wild-type rhodopsin content shown in Table II.

The error caused by the nonrandom orientation of rhodopsin chromophores in fly rhabdomeres can be estimated from the expression for the dichroic absorption by a rhabdomeral microvillus derived by Moody and Parriss (1961). These authors derived their expression under the assumption that the pigment molecules are distributed uniformly over the cylindrical surface of the microvillus and are oriented randomly within that surface. Kirschfeld (1969) has argued that dichroic ratios derived from the Moody-Parriss expression are consistent with the available electrophysiological data on the polarization sensitivity of fly rhabdomeres. Comparing the Moody-Parriss expression with one for randomly oriented chromophores, one can show that for unpolarized light propagating along the optic axis of the rhabdomere, the assumption of random orientation leads to an overestimation of rhodopsin content by nine-eighths. Because this error affects both the wild-type and mutant pigment levels, it does not affect the relative rhodopsin content. Hence, no corrections were applied for this error in Table II.

Calculation of Power Spectra

Bump parameters were analyzed at two or more light intensities for each cell. The protocol for the collection of steady state noise data was the same for all intensities. The computer was programmed to turn on the light stimulus, wait 5 s for the response to reach steady state, and then sample for 14 s. The time between stimuli was determined beforehand as the shortest time required to "dark-adapt" the cell. The cell was considered dark-adapted if successive stimuli of equal intensity yielded responses of the same amplitude. Thus, the dark-adaptation time ranged from 2 min at the highest intensities to 30 s at the lowest intensities. Because the bump parameters depended on the level of light adaptation, it was important to maintain the same adaptation level throughout the experiment.

The stimulus control, data collection, and data analysis were all done on-line with the PDP 11/03 computer. Because digital sampling was necessary to calculate the power spectrum, several steps were taken to avoid aliasing of the data. First, the data were filtered to restrict the bandwidth to <100 Hz. Second, the results for any given stimulus were obtained by averaging overlapping ensembles of 16 consecutive data points sampled at 448-μs intervals into a bin of 2,048 points. This procedure corresponded to a relatively slow sampling rate of 140 Hz. The data were cosine-tapered to correct for the rectangular shape of the sampling function and then Fourier-transformed. The square of voltage per hertz was then plotted against frequency to yield the power spectral density or power spectrum.

Noise Analysis

Quantum bumps can be identified as individual events only at relatively low stimulus intensities (Figs. 4 and 5); at higher intensities, they appear as noise superimposed on the mean response of the cell. The shot noise theory enables one to determine the average rate, amplitude, and duration of constituent events even when individual events are not resolvable.

A general theorem that relates experimentally measurable quantities to the microscopic parameters of the noise source is known as Campbell's theorem (Campbell, 1909*a*, *b*; Rice, 1944). Knight (1972) has shown that Campbell's theorem can be reduced to:

$$\bar{V} = \nu a T, \tag{1}$$

$$\sigma^2 = \nu a^2 T, \tag{2}$$

where $\bar{V}$ is the mean voltage, σ^2 is the variance, ν is the bump rate, a is the bump amplitude, and T is the bump duration. These expressions provide two of the three simultaneous equations needed to determine the three bump parameters, a, ν, and T. The third equation, which specifies the parameter T from the power spectrum, is obtained as outlined below.

Wong and Knight (1980) and Wong et al. (1982) have shown, in their treatment of *Limulus* eccentric and ventral photoreceptors, that the following form of the gamma distribution function describes the shape of a single bump reasonably well:

$$g(t) = \Gamma = \frac{1}{n!T}(t/\tau)^n \exp(-t/\tau), \tag{3}$$

where $g(t)$ is the bump waveform, t is time, τ is the time constant, and n is an integer. The square of the bump shape in the frequency domain, obtained by the Fourier transformation of Eq. 3, is given by the expression:

$$|g^2(f)| = \frac{1}{[1 + (2\pi f\tau)^2]^m}, \tag{4}$$

where f is frequency in hertz and $m = n + 1$. This expression is directly proportional to the power spectral density. That is,

$$S_v(f) = 2\nu|g^2(f)| = \frac{2\nu}{[1 + (2\pi f\tau)^2]^m}. \quad (5)$$

Thus, fitting the experimentally determined power spectral density to Eq. 5 yields parameters m and τ. These values are then used to determine the average bump duration, T, from the following expression, derived directly from Campbell's theorem (see Knight, 1972, for derivation):

$$T = \frac{\tau(n!)^2 2^{2n+1}}{(2n)!}. \quad (6)$$

Once the values of m, τ, and T are known, the theoretical bump waveform, $g(t)$, can be determined as a function of time from Eq. 3.

EGTA Injection Experiments

Recording electrodes filled with 0.05 M EGTA, 2 M KAc, and 0.3 M HEPES buffer, pH 7.0, were used in these experiments. Current pulses of −0.5 nA, lasting 30–120 s, electrophoresed the EGTA into the cell. Two types of control experiments were carried out. In one, EGTA in the electrode was replaced with SO_4^{2-} to exclude nonspecific effects of injecting divalent anions. In the other, electrodes filled with the normal recording electrolyte, 2 M KAc, and 0.3 M HEPES buffer, pH 7.0, were used to exclude the effects of current injection itself.

RESULTS

Receptor Responses

The receptor potentials of photoreceptors of the *nina* mutants differed from those of wild type in at least two ways. They lacked the PDA (Fig. 1) and displayed substantially reduced sensitivity to light. Fig. 3 shows receptor potential amplitudes plotted against log relative stimulus intensity for wild type, several allelic mutants of *ninaE* (*P318*, *P332*, *P334*, and *P352*), and a *ninaD* mutant, *P246*. The amplitudes were measured from baseline to the steady state portion of the receptor potential, usually several times, beginning at 5 s after the onset of the stimulus. The only obvious effect of the mutations is a shift of the curves to higher intensities, with little change in shape. The receptor potentials of all the mutants apparently reached the same saturation level of ~23 mV as in wild type, with the exception of $ninaE^{P334}$ and $ninaE^{P352}$. In these two mutants, even the highest available stimulus intensity was not sufficient to generate large enough responses to approach saturation. In addition to these differences in the macroscopic properties of the receptor potential, the *nina* mutants displayed strikingly larger light-induced bumps (Fig. 4).

Passive Electrical Properties

The passive electrical properties of the photoreceptor membrane were examined to determine whether any changes in these properties could contribute to the mutant response properties. Table I shows the experimentally determined input resistance, capacitance, resting potential, and the membrane surface area de-

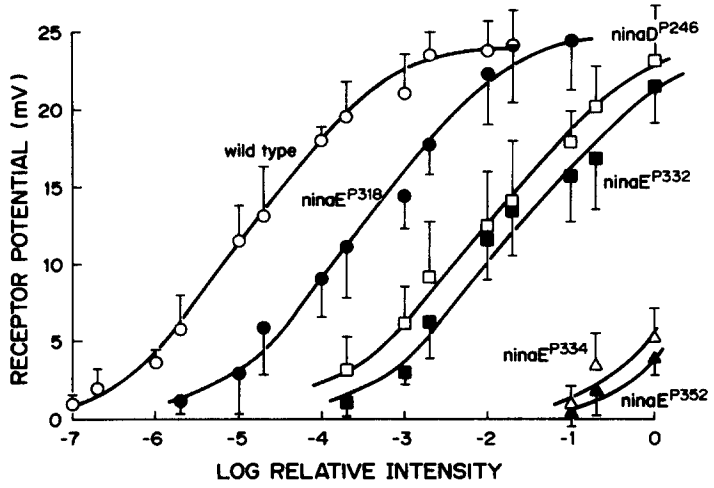

FIGURE 3. Comparison of semilog plots of the receptor potential amplitudes vs. stimulus intensity for wild type and mutants. Amplitudes were measured from baseline to the steady state portion of the receptor potential. The points were fitted by the relationship: $V = I/(I + \sigma)$, where σ is the intensity at half-maximal amplitude. The vertical bars are standard deviations based on the following sample sizes, n: wild type, 27; *ninaE*^{P318}, 8; *ninaD*^{P246}, 15; *ninaE*^{P332}, 17; *ninaE*^{P334}, 9; *ninaE*^{P352}, 6.

duced from the membrane capacitance for wild-type flies, five different *ninaE* mutants, and a *ninaD* mutant.

As can be seen in Table I, there was no significant difference in the resting potentials among the flies studied. The input resistance was also about the same for wild type, *ninaD*^{P246}, *ninaE*^{P318}, and *ninaE*^{P332}, whereas the more severe *ninaE* mutants, *P350*, *P334*, and *P352*, had somewhat greater resistances. For a given

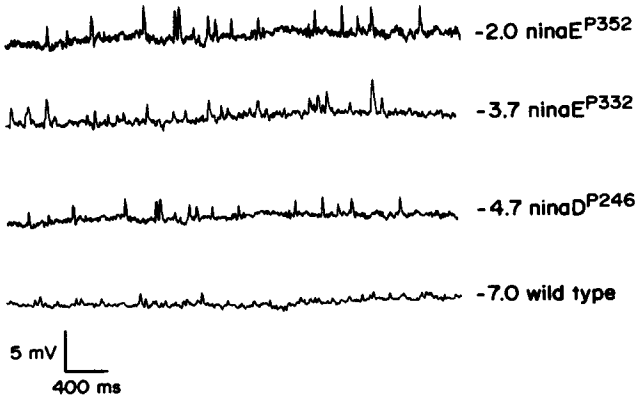

FIGURE 4. Intracellularly recorded responses of an R1–6 photoreceptor of *ninaE*^{P352}, *ninaE*^{P332}, *ninaD*^{P246}, and wild type during continuous stimulation with light of the relative log intensities indicated. For each class of fly, the light intensity was adjusted such that single bumps could be easily resolved. Note that the bump amplitude is greatest in *ninaE*^{P352} and smallest in wild type.

TABLE I

Passive Electrical Properties of Photoreceptor Membrane

Allele	Number of cells	Resting potential	Input resistance (mean ± SD)	Membrane capacitance	Deduced membrane surface area
		mV	*MΩ*	*× 10⁻¹² F*	*μm²*
Wild type	11	31.6±3.8	31.0±4.4	102±11	10,200
ninaE^{P318}	5	30.4±4.1	28.0±3.1	120±22	12,000
ninaD^{P246}	7	32.2±3.1	32.8±8.1	100±8	10,000
ninaE^{P332}	7	32.0±3.6	29.5±5.0	112±12	11,200
ninaE^{P350}	3	31.7±2.9	52.1±3.9	44±9	4,800
ninaE^{P334}	6	31.3±3.2	49.1±4.5	22±4	2,200
ninaE^{P352}	5	29.6±2.3	56.7±6.6	17±3	1,700

photocurrent, a voltage response is proportional to the input resistance. Thus, an increase in input resistance would give rise to a larger voltage response even in the absence of any increase in the light-evoked receptor current. However, even in the most severely affected mutants, *P334* and *P352*, the input resistance increased by only ~80% (Table I), whereas the bump amplitude increased by ~400% (Table II). Moreover, increases in bump amplitude of 280 and 350% were seen in *ninaD*^{P246} and *ninaE*^{P332}, respectively (Table II), even though there was no significant change in input resistance in these mutants (Table I).

The membrane capacitance of the mutant photoreceptors did not differ significantly from those of wild type, except in the severe *ninaE* mutants, *P350*, *P334*, and *P352*, all of which had considerably reduced membrane capacitances. The smallest capacitance observed was ~17% that of wild type. The surface areas of the photoreceptor membranes were estimated from the membrane capacitances, assuming that the specific capacitance of the membrane is ~1 $\mu F/cm^2$. These are also shown in Table I.

Electrophysiological Estimate of the Number of Rhodopsin Molecules

Although previous studies (Stephenson et al., 1983) had indicated that the rhodopsin level is extremely low in many of the *nina* mutants, the methods the previous investigators used did not allow determinations of rhodopsin levels

TABLE II

Rhodopsin Content and Bump Amplitude

Allele	Number of cells	Intensity of 5-ms flash		Number of rhodopsin molecules	Bump amplitude
		Relative	Absolute (mean ± SD)		
			photons/cm²		*mV*
Wild type	11	−5.7	$1.3\pm0.4\times10^{8}$	1.3×10^{8}	1.0±0.4
ninaE^{P318}	3	−4.0	$6.3\pm0.8\times10^{9}$	2×10^{6}	2.1±0.4
ninaD^{P246}	7	−3.7	$1.3\pm0.2\times10^{9}$	1×10^{6}	3.9±0.6
ninaE^{P332}	7	−2.7	$1.3\pm0.4\times10^{10}$	1×10^{5}	4.6±1.5
ninaE^{P334}	6	−0.4	$2.5\pm0.7\times10^{13}$	500	4.8±1.1
ninaE^{P352}	5	−0.0	$6.3\pm0.7\times10^{13}$	210	5.0±0.9

beyond ~2 log units below the wild-type level. To overcome this problem, the amount of rhodopsin in a R1–6 photoreceptor was determined in this study from the intensity of light needed to induce, on the average, one bump in the R1–6 photoreceptor (Lisman and Bering, 1977; Materials and Methods).

By adjusting the intensity of 5-ms yellow stimulus flashes, it was possible to obtain records in which individual bumps could be clearly resolved (see Fig. 5). Table II shows the stimulus intensity needed to generate one bump in the R1–6 photoreceptor and the amount of rhodopsin calculated from the intensity for each class of fly studied. The uncorrected rhodopsin content in the R1–6 photoreceptor ranged from $\sim 10^8$ molecules in wild-type flies to ~210 in *ninaE*^{P352}, a reduction of nearly six orders of magnitude. As explained in the Materials and Methods, the use of the present method leads to an underestimate of the wild-type rhodopsin content by ~30% but does not affect the mutant

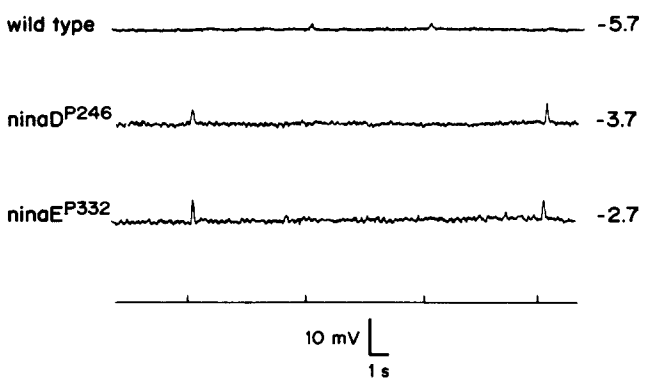

FIGURE 5. Representative records used to determine the rhodopsin content in the mutant and wild-type photoreceptors. The intensity of 5-ms light flashes was adjusted to yield a single bump one-third to two-thirds of the time. The bottom trace is the light monitor.

pigment contents. A correction for this error was incorporated into the wild-type pigment level shown in Table II.

Properties of Single Bumps

The amplitudes of single bumps, bump latency, and bump latency dispersion were determined from the same set of records obtained for the determination of the rhodopsin content. Care was taken to select records that yielded no more than one bump in response to any given stimulus. Otherwise, it was difficult to resolve individual bumps because of the very small latency dispersion (see below). The bump amplitudes determined in these experiments are displayed in Table II. The latency of individual bumps was ~32.7 ± 5.7 ms (n = 453) for all flies studied. The latency dispersion was minimal in each class of fly examined.

Noise Analysis

A detailed analysis of the noise properties of receptor responses was carried out on two *nina* mutants, *ninaE*^{P332} and *ninaD*^{P246}, and the properties were compared

with those of wild type. These two mutants were chosen because of the similarity in their V–log I curves (Fig. 3) and in the amplitude and time course of the PDA (Stephenson et al., 1983). These results had suggested that the extent to which these mutations affect the physiology of the photoreceptor is similar, even though

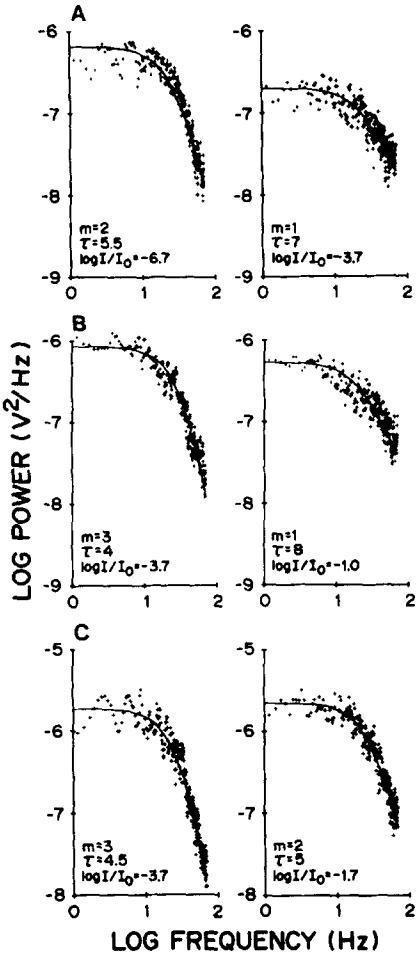

FIGURE 6. Representative double-log plots of power spectra obtained from wild-type (*A*), *ninaD*^{P246} (*B*), and *ninaE*^{P332} (*C*) photoreceptors at stimulus intensities that depolarize the cell by ~4–17 mV. The data were fitted by the following relationship: $|g^2(f)| = 1/[1 + (2\pi f\tau)^2]^m$. The values of m and τ determined from this fit are shown in the figure.

the mechanisms by which the rhodopsin content is reduced in the two mutants are very different (see Introduction).

Fig. 6 shows representative power spectra obtained from wild type (*A*), *ninaD*^{P246} (*B*), and *ninaE*^{P332} (*C*). Eq. 4 (Materials and Methods) was fitted to the spectra to determine the parameters τ and n, and the bump parameters ν, a, and

T were then calculated using Eqs. 1, 2, and 6. The variance, σ^2, was determined by taking the area under the power spectrum, and the steady state portion of the light-evoked response of the photoreceptor was taken to be the mean voltage, V. The parameter m of the mutant power spectra tended to be higher than that

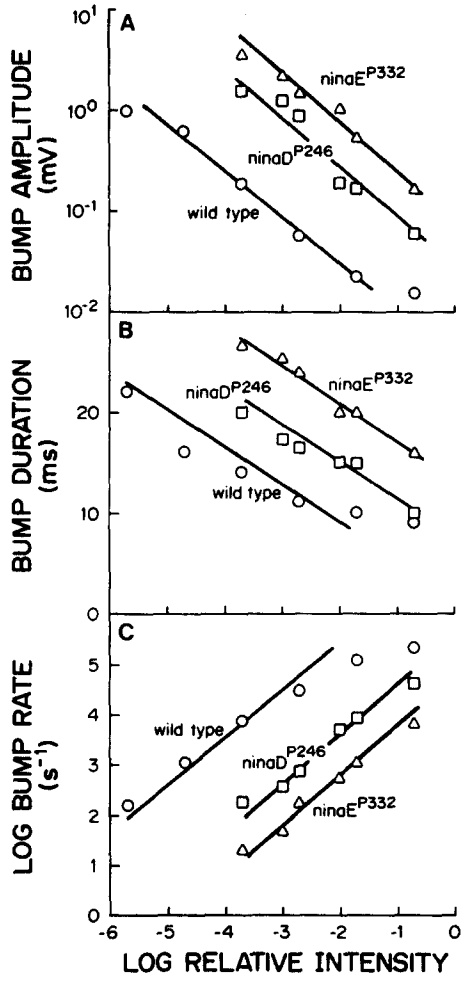

FIGURE 7. The bump parameters amplitude (A), duration (B), and rate (C), calculated from the steady state voltage noise and power spectra as described in the Materials and Methods, plotted against log light intensity for wild type, *ninaD*^{P246}, and *ninaE*^{P332}. It can be seen that for each bump parameter, the dependence on light intensity is similar across all classes of flies studied.

of wild type at any given depolarization level. This finding suggested that the shape of bumps underlying the larger-amplitude noise of mutants might be different from that of smaller wild-type bumps.

The average amplitude, duration, and rate of bumps obtained in noise analysis are plotted against log light intensity in Fig. 7 for the two mutants and wild type.

In all three sets of plots, mutant curves were shifted to higher intensities with respect to wild-type curves, reflecting the higher stimulus intensities needed to generate mutant bumps.

The bump amplitude decreased with increasing light intensity with a slope of about −0.6 for both wild type and the mutants in a double-log plot (Fig. 7*A*). The average bump duration, on the other hand, decreased with light intensity with a slope of about −3 in a semilog plot (Fig. 7*B*). In wild type, the duration approached a steady minimum value of ~10 ms at high light intensities.

The average bump rate increased with intensity with a slope of ~0.9 in a double-log plot for both wild type and the mutants (Fig. 7*C*). In wild type, the bump rate showed signs of saturation at a log relative intensity of about −3. The *ninaD* and *ninaE* curves were shifted to the right by ~2 and 3 log units,

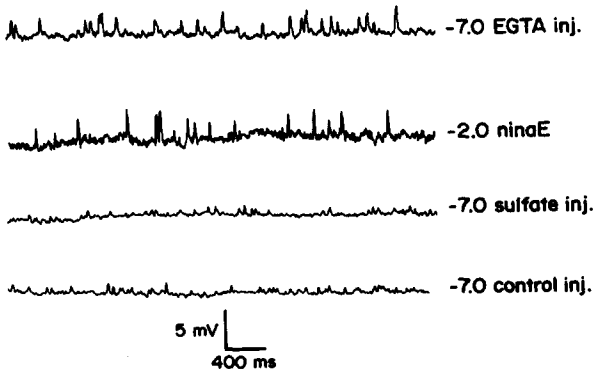

FIGURE 8. Responses of wild-type photoreceptors injected with EGTA (first trace), sulfate (third trace), and normal recording electrolyte (fourth trace) and of uninjected $ninaE^{P352}$ photoreceptors (second trace) during continuous stimulation with lights of the relative log intensities indicated. Light intensities were adjusted to yield easily resolvable single bumps. It can be seen that the injection of EGTA results in increasing the wild-type bump amplitude to the level seen in the mutant.

respectively, with respect to the wild-type curve. No evidence of saturation was observed in the mutant curves in the range of intensities studied.

Effects of Injecting the Calcium-Chelator EGTA

To test the possibility that calcium might play a role in the generation of the large bumps seen in the mutants, the intracellular free calcium concentration of the photoreceptor was buffered or reduced by electrophoretically injecting the calcium-chelating agent EGTA into the cell. As shown in Fig. 8, the bumps recorded from wild-type photoreceptors injected with EGTA were significantly larger than those obtained in the two control experiments (see Materials and Methods). In fact, they were comparable in size to those of the *nina* mutants. In the case of *Limulus* photoreceptors, reducing the internal free calcium has been shown to increase the latency and latency dispersion of bumps (Lisman and Brown, 1975; Martinez and Srebro, 1976). We compare in Fig. 9 the time courses of receptor responses to 5-ms flashes of several different intensities

obtained from the *ninaE*^{P332} photoreceptor, the EGTA-injected wild-type photoreceptor, and the uninjected wild-type photoreceptor. The latency and waveform of the responses of the *ninaE* and uninjected wild-type photoreceptors were very similar (Fig. 9, top and bottom traces). By contrast, the responses of the EGTA-injected photoreceptor were much slower in time course and had much longer latencies (Fig. 9, middle traces). Thus, EGTA injection appears to mimic

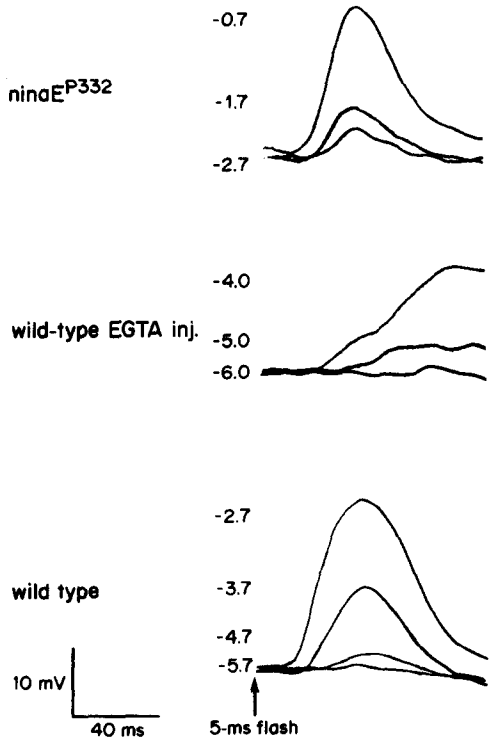

FIGURE 9. Receptor potentials recorded from *ninaA*^{P332} (*A*), EGTA-injected wild-type (*B*), and uninjected wild-type control (*C*) photoreceptors. In each case, several responses evoked by 5-ms flashes of different intensities (relative log intensities shown) are superimposed in the figure. The records are displayed at high sweep speed to demonstrate the differences in response latency and kinetics of the EGTA-injected photoreceptors.

the *nina* mutations in the way it affects the bump amplitude, but not in the way it affects the response latency and latency dispersion.

DISCUSSION

In this investigation, we wanted to address the following questions: (*a*) whether or not the *nina* mutations have any effect on the physiological parameters of bumps, (*b*) if they do have an effect, whether the effect can be attributed to an alteration in the opsin protein or simply to the low rhodopsin content, and (*c*) whether or not the mechanisms of bump generation and adaptation still operate under conditions in which individual rhodopsin molecules are physically well

separated from each other. To address these questions, it was necessary to determine the amount of rhodopsin in each mutant.

The number of rhodopsin molecules in the R1–6 photoreceptor of wild-type *Drosophila* was determined by an electrophysiological method to be ~10^8 (Table II). This number is subject to considerable uncertainty because of the difficulty in estimating the number of photons incident on the photoreceptor (see Materials and Methods). Accordingly, two other methods were used. One of these is based on the number of membrane particles seen in the rhabdomeric membrane in freeze-fracture electron microscopy. Assuming that the majority of the rhabdomeric membrane particles are, or are associated with, single rhodopsin molecules, the number of rhodopsin molecules was estimated from the product of the rhabdomeric particle density (~2,960 particles/μm^2, Schinz et al., 1982) and the rhabdomeric surface area (9,500 μm^2, Schinz et al., 1977) to be ~3×10^7 molecules per R1–6 cell. It is estimated that rhodopsin actually constitutes only

TABLE III

Calculated Density of Rhodopsin in the Rhabdomeres

Allele	Corrected number of rhodopsin molecules	Rhabdomeric membrane area	Rhodopsin density in rhabdomeres	Area occupied by one rhodopsin molecule
		μm^2	μm^{-2}	μm^2
Wild type	4×10^7	9,300	4,300	2.3×10^{-4}
ninaE^{P318}	6×10^5	11,100	54	1.8×10^{-2}
ninaD^{P246}	3×10^5	9,100	33	3.0×10^{-2}
ninaE^{P332}	3×10^4	10,300	2.9	0.34
ninaE^{P334}	150	1,300	0.12	8.7
ninaE^{P352}	65	800	0.081	12.3

~65% of the membrane particles in fly rhabdomeres (Larrivee, 1979; Pak et al., 1980; Schwemer and Henning, 1984). We made no attempts to correct for the possible presence of nonrhodopsin particles in the rhabdomeric membrane.

In another method, the spectrophotometrically determined absorbance of metarhodopsin in the living fly was used to obtain the amount of rhodopsin. As shown in detail in the Appendix, this method yielded a value of ~$4–5 \times 10^7$ molecules per R1–6 photoreceptor. The results obtained by the two methods agree reasonably well. Accordingly, we have taken the average of these two determinations (i.e., ~4×10^7) to be a reasonable estimate of the rhodopsin content in the wild-type photoreceptor, and appropriate corrections were applied to the electrophysiological results displayed in Table II. The corrected rhodopsin contents are shown in Table III.

The electrophysiological method, however, is exquisitely sensitive for determining the amount of rhodopsin in the mutants relative to that in the wild-type photoreceptor. Thus, the technique enabled us to determine the relative rhodopsin contents nearly 6 log units below that of wild type (Table II). The techniques applied previously for this purpose, by contrast, were reliable for a decrease in pigment levels of only up to ~2 log units (Stephenson et al., 1983).

The method, however, assumes that the quantum efficiency of rhodopsin isomerization and the rhodopsin extinction coefficient are not altered in the mutants. Insofar as these values have not been determined for any of the mutants, the results of these measurements must be interpreted with caution. It should be noted, however, that no anomalous alterations in the sensitivity or other physiological parameters of the photoreceptor that might indicate gross changes in these values have been observed in any of the mutants studied.

The total cell membrane surface area of the wild-type R1–6 photoreceptor deduced from the membrane capacitance measurements is ~10,200 μm^2 (Table I). This area is greatly reduced in severely affected *ninaE* mutants (Table I). From previous electron-microscopic studies of wild-type photoreceptors, the total membrane surface area of an R1–6 photoreceptor has been estimated to be ~10,000 μm^2, 8–9% of which is contributed by the nonrhabdomeric cell surface membrane (Schinz, R., and R. S. Stephenson, unpublished observations). Studies at the light-microscopic level show that strong *ninaE* mutations severely reduce rhabdomere size without noticeably affecting cell body size (Leonard, D., unpublished observations).

Thus, the available data suggest (*a*) that electrophysiologically derived estimates of cell surface membrane areas are in good agreement with available histological estimates, (*b*) that ~900 μm^2 (~9%) of the electrophysiologically derived total membrane surface area of the wild-type photoreceptor is contributed by the nonrhabdomeric cell surface membrane, and (*c*) that this area is not significantly altered in the mutants. Accordingly, we estimated the area of the rhabdomeric membrane in both wild type and the mutants by subtracting 900 μm^2 from the electrophysiologically derived total cell membrane area (Table I). The results are shown in the third column of Table III. Also shown in the table are the surface density of rhodopsin (fourth column) and the reciprocal of the density (fifth column) for flies of each genotype.

The last set of numbers corresponds to the average size of a patch of rhabdomeric membrane occupied by one rhodopsin molecule. One might ask how these numbers compare with the surface area of a single microvillus in the rhabdomere. The cross-sectional diameter of a microvillus is ~3.8×10^{-2} μm (Schinz, R., unpublished data). The lengths of microvilli in a given rhabdomere vary considerably, depending on their location. The lengths of the largest microvilli, which for our purpose, can be approximated by the cross-sectional diameter of the rhabdomere, are ~1.6 μm in wild type, ~1.2 μm in *P332*, and smaller still in more severely affected *ninaE* mutants (Leonard, D., unpublished observations). Thus, the surface area of the largest microvilli is ~0.18 μm^2 in *P332* and is smaller than that in *P334* or *P352*. It may be noted that for the three most severe *ninaE* mutants, *P332*, *P334*, and *P352*, the average size of a patch of membrane occupied by one rhodopsin molecule is considerably larger than the surface area of the largest microvilli. Since most of the microvilli in the rhabdomere are considerably shorter than those considered above, the above observation implies that the rhabdomeric membrane of these mutants, particularly the latter two, is so sparsely populated by rhodopsin molecules that most of the microvilli in the rhabdomere are devoid of functional rhodopsin molecules, providing little possibility of rhodopsin-rhodopsin interactions.

A surprising finding of this investigation is that the photoreceptor of even the most severely affected mutant investigated can respond to light with apparently healthy bumps (Fig. 4). Moreover, the latency and latency dispersion of single bumps in all mutants investigated are similar to those of wild type. Thus, the basic mechanism of bump generation does not appear to be altered even in the most severely affected *nina* mutants examined. The results strongly suggest that the phototransduction initiated by each rhodopsin molecule proceeds independently of interaction with other rhodopsin molecules.

The results of noise analysis, carried out on $ninaD^{P246}$, $ninaE^{P332}$, and wild type at several stimulus intensities, show that the adapting bump model (Dodge et al., 1968) holds not only for the wild-type responses, in agreement with the earlier findings of Wu and Pak (1978), but also for the responses of the $ninaD^{P246}$ and $ninaE^{P332}$ mutants. As can be seen in Fig. 7, each of the three bump parameters of the mutants shows a dependence on the stimulus intensity that is similar to the corresponding wild-type parameter. That is, the bump rate increases approximately linearly with light intensity in both the mutants and wild type, and the mutant bump duration and amplitude adapt to increasing light intensity in the same manner as in wild type. Since the number of functional rhodopsin molecules in the mutant $ninaE^{P332}$ is sufficiently small to preclude any significant contacts or interactions among these molecules (see Table III), the above results suggest that a single rhodopsin molecule is capable of initiating and sustaining not only the excitation but also the adaptation process in the absence of interactions with other rhodopsin molecules.

Our results of noise analysis on wild-type flies are qualitatively similar to those of Wu and Pak (1978). However, they do differ from the earlier results in a number of aspects. The amplitudes of bumps are about an order of magnitude larger, and they depend on the stimulus intensity less strongly than reported previously. Moreover, although the earlier study had indicated that the bump duration is relatively constant with stimulus intensity, the present results suggest that it does decrease with stimulus intensity (Fig. 7, Results). The dependence on stimulus intensity, however, is much smaller than that reported for *Limulus* (Wong et al., 1982). The exact cause of the discrepancy cannot yet be ascertained. However, the most likely cause appears to be the difference in the way flies were prepared for recording. In the present work, flies were kept intact during recording, except for a small hole made in the cornea to introduce the electrode (Material and Methods). By contrast, in the earlier work (Wu and Pak, 1975), a substantial portion of the head was sliced off to expose the photoreceptor layer, and the sliced head was immersed in saline.

The mutant bumps differ from those of wild type in their amplitude and sensitivity to light, and possibly also in their shape. The difference in sensitivity arises because of the low rhodopsin content in the mutants and manifests itself as a shift of the mutant curves to higher intensities in plots of mutant response properties against stimulus intensity (Figs. 3 and 7). Since, in the adapting bump model, the bump rate is directly related to the rate at which rhodopsin molecules are excited, a shift in the mutant bump rate curve should correspond to a change in the number of functional rhodopsin molecules. In fact, the bump rate curves of $ninaD^{P246}$ and $ninaE^{P332}$ were found to be shifted to higher intensities by ~1.9

and 2.9 log units, respectively (Fig. 7*C*), whereas the rhodopsin contents were reduced by 2.1 and 3.1 log units, respectively (Table II).

Probably the most striking difference between the mutant and wild-type bumps is their amplitude (Figs. 4 and 5, Table II). Although the increase in membrane resistance does contribute to the larger amplitude somewhat, it does not account for the magnitude of increase seen in the mutants (Table II). The degree of increase in bump amplitude seen in the two mutants, *ninaD* and *ninaE*, is very similar. Moreover, the sensitivity of the responses is also altered in a similar way in the two mutants. No changes in the physiological parameters of the photoreceptor that could be ascribed only to the *ninaE* mutations have been detected in this investigation. Insofar as the only notable common consequence of the two mutations is a severe decrease in the amount of functional rhodopsin, the amplitude increase and sensitivity decrease are both probably direct consequences of decreased rhodopsin content.

The *ninaE* gene, however, encodes the opsin protein in R1–6 photoreceptors (O'Tousa et al., 1985; Zuker et al., 1985). Depending on its site, a mutation in this gene could give rise to (*a*) a varying degree of rhodopsin depletion, or (*b*) physiological defects that cannot be explained by rhodopsin depletion alone, or (*c*) some combination of the two. The *ninaE* mutants analyzed here apparently belong to the first class. The reason most *ninaE* mutants isolated to date are apparently of this type may be that the mutant selection scheme based on underdeveloped PDAs favors the isolation of mutants with greatly decreased rhodopsin contents.

Because of the technical difficulty involved, the present analysis of bumps was carried out using voltage noise, rather than current noise. Unfortunately, the use of voltage noise introduces a number of unavoidable errors. First, because the driving force for the receptor potential decreases as the membrane voltage approaches the reversal potential, the bumps do not summate linearly, as required by Campbell's theorem. Second, not only light-induced conductance changes, but also a number of voltage-dependent conductance changes, contribute to voltage noise. Nevertheless, a comparison of bump properties carried out at similar depolarization levels should still be valid, because the contribution of these errors to wild-type and mutant responses ought to be the same.

Buffering or reducing the internal or external calcium concentration has been shown to increase the steady state amplitude of the receptor potential in *Limulus* (Lisman and Brown, 1975) and *Drosophila* (Wilcox, 1980), as well as the noise amplitude in *Limulus* (Wong et al., 1982). We sought to determine whether this effect of calcium might be related to the observed effects of *nina* mutations on bumps. Iontophoretic injection of the calcium-chelator EGTA, carried out to test this hypothesis, did mimic the effect of the mutations on the bump amplitude (Fig. 8). However, it also slowed down the response kinetics (Fig. 9), while the mutations had no such effect on the kinetics. Thus, the observed effects of the mutations do not appear to be mediated solely, if at all, through the regulation of the internal calcium concentration.

Nonetheless, the above study provides some interesting insights. For example, it supports the idea that the bump amplitude and bump kinetics are mediated by

separate processes, even though injecting EGTA affects both, because the *nina* mutations affect the former but not the latter. In addition, if the mutations and calcium chelation increase the bump amplitude by the same mechanism, the EGTA-injection results would suggest that one site of calcium action is at or near the pigment level.

Finally, a possible, though rather simplistic, explanation for the larger bumps seen in the mutants can be stated as follows. Suppose one makes the assumptions that the *nina* mutations reduce the number of rhodopsin molecules but not the amount of the enzymes involved in the subsequent steps of transduction, and that nonactivated rhodopsin molecules normally compete with activated rhodopsin molecules for the available enzyme machinery. Then one would expect more enzymes to be available per photoactivated rhodopsin molecule in the mutants than in wild type. Under these conditions, larger bumps would be produced in the mutants because more enzymes are activated and more channels are opened for each rhodopsin molecule activated.

APPENDIX

Determination of Rhodopsin Content from Absorbance Measurements on the Deep Pseudopupil

Measurements were carried out on the deep pseudopupil of living flies. The deep pseudopupil is a superposition of virtual images of rhabdomere tips in many neighboring ommatidia and appears as seven bright or dark spots arranged in a typical trapezoidal pattern in transmitted light (Franceschini, 1972). The measurements consisted of determinations of absorbance differences at ~580 nm between blue-adapted and yellow-adapted photoreceptors, measured through a small, rectangular window that just surrounds the deep pseudopupil with the test beam coming through the back of the eye. Since rhodopsin absorbs maximally at ~480 nm and metarhodopsin at ~580 nm, the measurements represent the maximal absorbance of metarhodopsin in R1–6 rhabdomeres, when essentially all of the rhodopsin has been converted to metarhodopsin. The metarhodopsin, rather than the rhodopsin, absorbance is used in this exercise, because it has a significantly larger extinction coefficient than rhodopsin. However, only ~60% of the light falling on the rectangular window passes through rhabdomeres 1–6. Therefore, the measured absorbance difference is not the actual metarhodopsin absorbance difference in the rhabdomeres, and it is necessary to determine the latter from the former, as shown below, to calculate the concentration of visual pigment in R1–6 rhabdomeres.

The measured absorbance difference, ΔA_m, is given by

$$\Delta A_m = A_m(B) - A_m(Y), \tag{1}$$

where $A_m(B)$ is the absorbance measured through the rectangular window after blue adaptation, and $A_m(Y)$ is the absorbance measured after yellow adaptation. Since the absorbances are defined by

$$A_m(B) = -\log[I_t(B)/I_i] \tag{2}$$

and

$$A_m(Y) = -\log[I_t(Y)/I_i], \tag{3}$$

where I_i is the intensity of incident light, $I_t(B)$ is the intensity of transmitted light after

blue adaptation, and $I_t(Y)$ is the intensity of transmitted light after yellow adaptation, we obtain

$$\Delta A_m = \log[I_t(Y)/I_t(B)]. \tag{4}$$

The transmitted intensities can be related to the actual absorbances of rhabdomeres by the following equations:

$$I(B) = I_i(1 - f)10^{-A_n} + I_i f 10^{-A(B)} \tag{5}$$

and

$$I(Y) = I_i(1 - f)10^{-A_n} + I_i f 10^{-A(Y)}, \tag{6}$$

where f is the fraction of test light passing through R1–6 rhabdomeres, $A(B)$ is the absorbance of R1–6 rhabdomeres after blue adaptation, $A(Y)$ is the absorbance of R1–6 rhabdomeres after yellow adaptation, and A_n is the absorbance of the nonrhabdomeric region in the measuring beam. Note that A_n is taken to be the same after both blue and yellow adaptations because no light-sensitive pigments are assumed to be present in the nonrhabdomeric portions of eye tissue intercepted by the measuring beam. Substituting Eqs. 5 and 6 into Eq. 4, we obtain

$$\Delta A_m = \log\left[\frac{(1 - f)10^{-\delta} + f}{(1 - f)10^{-\delta} + f10^{-\Delta A}}\right], \tag{7}$$

where $\delta = A_n - A(Y)$ and $\Delta A = A(B) - A(Y)$. Solving for ΔA, we obtain

$$\Delta A = \log\left\{\frac{f}{10^{-\Delta A_m}[(1 - f)10^{-\delta} + f] - (1 - f)10^{-\delta}}\right\}. \tag{8}$$

This is the expression for the difference in absorbance of blue- and yellow-adapted R1–6 rhabdomeres, measured at 580 nm. In the special case where $\delta = 0$, the above expression reduces to

$$\Delta A = \log\left[\frac{f}{10^{-\Delta A_m} - (1 - f)}\right]. \tag{9}$$

Eq. 9 is valid if the absorbance of R1–6 rhabdomeres at 580 nm after yellow adaptation is the same as the absorbance of the surrounding nonrhabdomeric medium in the measuring beam. In reality, R1–6 rhabdomeres transmit more 580-nm light than the surrounding medium after yellow adaptation, i.e., $\delta > 0$. Fortunately, ΔA is not a strongly dependent function of δ. Thus, for each change in δ of 0.1, ΔA changes by only ~10%. For the present application, we have taken $\delta = 0.1$, $f = 0.6$, and $\Delta A_m = 0.158$ (Scavarda et al., 1983). Thus, we obtain

$$\Delta A = 0.27. \tag{10}$$

The number of rhodopsin molecules in a photoreceptor are then calculated from Beer's law, taking the molar extinction coefficient of metarhodopsin to be 56,000 liters/mol-cm (Ostroy, 1978), the length of the R1–6 rhabdomere, $\sim 6 \times 10^{-3}$ cm, to be the pathlength of the test light, and the rhabdomeric volume of an R1–6 photoreceptor to be $\sim 10^{-13}$ liter. We obtain

$$n \approx 4.9 \times 10^7 \text{ rhodopsin molecules/R1–6 photoreceptor.}$$

If we had taken δ to be zero, this value would have been ~10% larger, and if we had taken it to be 0.2, the value would have been ~10% smaller. If we now correct for the

polarization absorption by rhabdomeres, as outlined in the Materials and Methods, the corrected number is

$$n_c \approx 4.4 \times 10^7 \text{ rhodopsin molecules/R1–6 photoreceptor.}$$

We thank Drs. J. O'Tousa, S. Nakajima, L. Pinto, and T. Goldsmith for helpful discussions and Ms. L. L. Randall for carefully proofreading the manuscript. We also thank Drs. R. Schinz and R. S. Stephenson, Ms. D. Leonard, and Mr. Q. Pye for their permission to discuss their unpublished data.

This work was supported by grant EY00033 from the National Eye Institute, National Institutes of Health (W.L.P.), and by training grant EY07008 from the National Eye Institute to Purdue University (E.J.).

Original version received 9 January 1986 and accepted version received 17 July 1986.

REFERENCES

Baylor, D. A., T. D. Lamb, and K.-Y. Yau. 1979. Responses of retinal rods to single photons. *Journal of Physiology.* 228:589–611.

Brown, H. M., and M. C. Cornwall. 1975. Spectral correlates of a quasi-stable depolarization in barnacle photoreceptor following red light. *Journal of Physiology.* 248:555–578.

Campbell, N. 1909*a*. The study of discontinuous phenomena. *Proceedings of the Cambridge Philosophical Society.* 15:117–136.

Campbell, N. 1909*b*. Discontinuities in light emission. II. *Proceedings of the Cambridge Philosophical Society.* 15:513.

Cosens, D., and D. Briscoe. 1972. A switch phenomenon in the compound eye of the white-eyed mutant of *Drosophila melanogaster. Journal of Insect Physiology.* 18:627–632.

Dodge, F. A., Jr., B. W. Knight, and J. Toyoda. 1968. Voltage noise in *Limulus* visual cells. *Science.* 160:88–96.

Franceschini, N. 1972. Pupil and pseudopupil in the compound eye of *Drosophila. In* Information Processing in the Visual Systems of Arthropods. R. Wehner, editor. Springer-Verlag, Berlin. 75–82.

Fuortes, M. G. F., and S. Yeandle. 1964. Probability of occurrence of discrete potential waves in the eye of *Limulus. Journal of General Physiology.* 47:443–463.

Hardie, R. C. 1979. Electrophysiological analysis of fly retina. I. Comparative properties of R1–6 and R7 and 8. *Journal of Comparative Physiology A.* 129:19–33.

Harris, W. A., W. S. Stark, and J. A. Walker. 1976. Genetic dissection of the photoreceptor system in the compound eye of *Drosophila melanogaster. Journal of Physiology.* 256:415–439.

Hillman, P., S. Hochstein, and B. Minke. 1972. A visual pigment with two physiologically active stable states. *Science.* 175:1486–1488.

Kirschfeld, K. 1969. Absorption properties of photopigments in single rods, cones and rhabdomeres. *Proceedings of the International School of Physics E. Fermi.* 43:116–136.

Knight, B. W., Jr. 1972. Some point processes in motor and sensory neurophysiology. *In* Stochastic Point Processes. P. A. W. Lewis, editor. John Wiley & Sons, Inc., New York. 732–755.

Larrivee, D. C. 1979. A biochemical analysis of the *Drosophila* rhabdomere and its extracellular environment. Ph.D. Thesis. Purdue University, West Lafayette, IN. 110–153.

Lillywhite, P. G. 1977. Single photon signals and transduction in an insect eye. *Journal of Comparative Physiology.* 122:189–200.

Lindsley, D. L., and E. H. Grell. 1968. Genetic Variations of *Drosophila melanogaster*. Carnegie Institution of Washington, Washington, DC. 266–267.

Lisman, J. E., and H. Bering. 1977. Electrophysiological measurement of the number of rhodopsin molecules in single *Limulus* photoreceptors. *Journal of General Physiology*. 70:621–633.

Lisman, J. E., and J. E. Brown. 1975. Effects of intracellular injection of calcium buffers on light adaptation in *Limulus* ventral photoreceptors. *Journal of General Physiology*. 66:489–506.

Martinez, J. M., and R. Srebro. 1976. Calcium and the control of discrete wave latency in the ventral photoreceptor of *Limulus*. *Journal of Physiology*. 261:535–562.

Moody, M. F., and J. R. Parriss. 1961. The discrimination of polarized light by *Octopus*: a behavioural and morphological study. *Zeitschrift für Vergleichende Physiologie*. 44:268–291.

Nolte, J., J. E. Brown, and T. G. Smith, Jr. 1968. A hyperpolarizing component of the receptor potential in the median ocellus of *Limulus*. *Science*. 162:677–679.

Ostroy, S. E. 1978. Characteristics of *Drosophila* rhodopsin in wild type and *norpA* vision transduction mutants. *Journal of General Physiology*. 72:717–732.

O'Tousa, J. E., W. Baehr, R. L. Martin, J. Hirsch, W. L. Pak, and M. L. Applebury. 1985. The Drosophila *ninaE* gene encodes an opsin. *Cell*. 40:839–850.

Pak, W. L. 1979. Study of photoreceptor function using *Drosophila* mutants. *In* Neurogenetics: Genetic Approaches to the Nervous System. X. Breakfield, editor. Elsevier/North-Holland, New York. 67–99.

Pak, W. L., S. K. Conrad, N. E. Kremer, D. C. Larrivee, R. H. Schinz, and F. Wong. 1980. Photoreceptor function. *In* Development and Neurobiology of *Drosophila*. O. Siddiqi, P. Babu, L. M. Hall, and J. C. Hall, editors. Plenum Publishing Corp., New York. 331–346.

Rall, W. 1960. Membrane potential transients and membrane time constant of motoneurons. *Experimental Neurology*. 2:503–532.

Rice, S. O. 1944. Mathematical analysis of random noise. *Bell Systems Technical Journal*. 23:282–332.

Rushton, W. A. H. 1961. The intensity factor in vision. *In* Light and Life. W. D. McElroy and H. B. Glass, editors. The Hopkins University Press, Baltimore, MD. 706–722.

Scavarda, N. J., J. O'Tousa, and W. L. Pak. 1983. *Drosophila* locus with gene-dosage effects on rhodopsin. *Proceedings of the National Academy of Sciences*. 80:4441–4445.

Schinz, R., S. E. Ostroy, and W. L. Pak. 1977. Freeze-fracture study of *Drosophila* rhabdomeric membrane. *Investigative Ophthalmology and Visual Science*. 16(Suppl.):146. (Abstr.)

Schinz, R. H., M.-V. C. Lo, D. C. Larrivee, and W. L. Pak. 1982. Freeze-fracture study of the *Drosophila* photoreceptor membrane: mutations affecting membrane particle density. *Journal of Cell Biology*. 93:961–969.

Schwemer, J., and U. Henning. 1984. Morphological correlates of visual pigment turnover in photoreceptors of the fly, *Calliphora erythrocephala*. *Cell and Tissue Research*. 236:293–303.

Stephenson, R. S., J. O'Tousa, N. J. Scavarda, L. L. Randall, and W. L. Pak. 1983. *Drosophila* mutants with reduced rhodopsin content. *In* The Biology of Photoreception. D. J. Cosens and D. Vince-Price, editors. Cambridge University Press, Cambridge, England. 477–501.

Steward, R., and C. Nusslein-Vohlard. 1986. The genetics of the *dorsal-Bicaudal-D* region of *Drosophila melanogaster*. *Genetics*. 113:665–678.

Wilcox, M. 1980. The ionic mechanism of the photoreceptor in mutant and wild type *Drosophila melanogaster*. Ph.D. Thesis. Purdue University, West Lafayette, IN. 143 pp.

Wong, F., and B. W. Knight. 1980. Adapting-bump model for eccentric cells of *Limulus*. *Journal of General Physiology*. 76:539–557.

Wong, F., B. W. Knight, and F. A. Dodge. 1982. Adapting bump model for ventral photoreceptors of *Limulus*. *Journal of General Physiology*. 79:1089–1113.

Wu, C.-F., and W. L. Pak. 1975. Quantal basis of photoreceptor spectral sensitivity of *Drosophila melanogaster*. *Journal of General Physiology*. 66:149–168.

Wu, C.-F., and W. L. Pak. 1978. Light-induced voltage noise in the photoreceptor of *Drosophila melanogaster*. *Journal of General Physiology*. 71:249–268.

Yeandle, S., and J. B Spiegler. 1973. Light-evoked discrete waves in the ventral nerve photoreceptor of *Limulus*. *Journal of General Physiology*. 61:552–571.

Zuker, C. S., A. F. Cowman, and G. M. Rubin. 1985. Isolation and structure of a rhodopsin gene from *D. melanogaster*. *Cell*. 40:851–858.